

## Photocatalytic Dehydrogenation of 2-Propanol on TiO<sub>2</sub>(110)

David Brinkley and Thomas Engel\*

Department of Chemistry, University of Washington, Box 351700, Seattle, Washington 98195-1700

Received: April 17, 1998; In Final Form: June 26, 1998

The photocatalytic production of acetone from 2-propanol and O<sub>2</sub> has been investigated on the TiO<sub>2</sub>(110) surface using molecular beam techniques. We have also studied the thermal reaction of 2-propanol with O<sub>2</sub> on this surface in the absence of light. We find that, in the absence of light, the probability of producing propene is greater than that for producing acetone, but the total probability for these reactions is less than 0.03 for a single collision of the incident molecule with the surface. This probability increases to 0.15 if band gap radiation is present on the surface, with acetone production being the dominant reaction channel. The maximum reaction probability is reached on a surface that has been preannealed in a vacuum to create oxygen vacancies. Fully oxidizing the surface reduces the probability to 0.08. The steady-state reaction yield is maximized at a surface temperature of 350 K and decreases to low values at 250 and 600 K. The yield is limited by desorption of acetone below 300 K and by the decrease in the surface coverage of reactants above 400 K. The absence of thermal reactivity and the significant photochemical reactivity is attributed to free-radical reactions initiated through electron trapping by adsorbed molecular oxygen. Our results suggest that the reaction proceeds through a mechanism in which holes are trapped by undissociated 2-propanol molecules.

### 1. Introduction

The potential use of wide band gap semiconductors to act as photocatalysts for the oxidation of organic substances has attracted significant attention in recent years.<sup>1,2</sup> TiO<sub>2</sub> is an excellent candidate for a photocatalyst because it is chemically quite stable under conditions in which surface redox reactions leading to contaminant degradation occur and because its band edge positions and gap width are compatible with a large number of desirable redox reactions.<sup>1,2</sup>

Most photocatalytic reaction studies reported in the literature have been carried out on TiO<sub>2</sub> colloidal suspensions or powders. Such studies are well-suited to maximizing yield and identifying reaction products. They have also proved useful in identifying reaction intermediates.<sup>1,3–6</sup> Complementary single-crystal studies have the potential to identify the influence of such parameters as surface structure, defect concentration, and the nature of the reactive intermediate that initiates the photooxidation reaction. The combination of fundamental studies on well-characterized surfaces in ultrahigh vacuum (UHV) and applied studies on colloidal suspensions and powders at higher pressures may allow an optimization of the reaction conditions and lead to an improvement in the formulation of photocatalysts. For example, recent work by Yates and co-workers<sup>7</sup> on single-crystal TiO<sub>2</sub> has indicated that molecularly adsorbed oxygen is essential for gas-phase photooxidation of trichloroethylene.<sup>8</sup> They also find that molecular oxygen is preferentially bound to oxygen vacancies at the surface.<sup>9</sup> This seems to imply that the photocatalytic activity can be enhanced by having certain types of defects in the near surface region.

We have chosen to investigate the photocatalytic oxidation of 2-propanol on TiO<sub>2</sub>(110) as a model reaction for several reasons. This reaction has been extensively studied recently

on a powder catalyst.<sup>10</sup> Single-crystal studies on the same reaction system will help to identify the similarities and differences between single crystals and powders. We have chosen to use the (110) orientation because this plane has the lowest surface energy relative to other planes in the rutile system. It will therefore be the dominant facet on microcrystalline powders if they have the equilibrium shape. Finally, the thermal reactions of the reactants and products in this system, 2-propanol, acetone, and water have all been studied on single-crystal and powder samples.<sup>11–13</sup> This information provides a background for understanding the different pathways encountered in thermal and photocatalytic reactions, as well as on single crystals and powders.

### 2. Experimental Section

Experiments were carried out in a UHV molecular beam surface scattering apparatus. The beam portion consists of two stages. The nozzle–skimmer chamber is pumped with an 5000 L s<sup>−1</sup> oil diffusion pump. This stage is followed by a collimation chamber pumped by a 700 L s<sup>−1</sup> oil diffusion pump. The UHV chamber is pumped by a 510 L s<sup>−1</sup> turbomolecular pump and a titanium sublimation pump. This chamber has capabilities for LEED, XPS, and ISS and allows dosing of a second gas through a pinhole aperture located close to the crystal. Two quadrupole mass spectrometers are mounted in the chamber. The first allows direct line-of-sight analysis of the beam. The mass spectrometer used to detect the scattered molecules is mounted in a separate chamber pumped by a 170 L s<sup>−1</sup> turbomolecular and a titanium sublimation pump. Apertures between the sample and the ionizer restrict the area sampled at the surface to a circle of approximately 3 mm. The ionizer is cooled with liquid nitrogen<sup>14</sup> to ensure a fast response time for condensable species such as 2-propanol, acetone, and water. The beam–detector angle is 90°, and the skimmer–surface and surface–ionizer distances are 21 and 5 cm, respectively. Typically, both the angle of incidence of the beam

\* Corresponding author. Telephone (206) 685-2330; Fax (206) 685-8665; E-mail engel@chem.washington.edu.

and the scattering angle were 45°. None of the results reported here were sensitive to variations of these angles.

The TiO<sub>2</sub>(110) single-crystal sample used in these studies is in the form of a 5 × 10 mm rectangle. It is held by tungsten wire spring clips to a tantalum plate slightly larger in size than the sample. To enhance thermal contact between the sample and the Ta plate, a 0.040 mm thick gold foil was inserted between the two. The sample could be cooled to 120 K using a copper braid connected to a liquid nitrogen reservoir and heated to 1000 K using electron bombardment to the back of the sample. Temperatures were measured using a chromel–alumel thermocouple fastened to an edge of the TiO<sub>2</sub> sample using a ceramic adhesive. Clean well-ordered surfaces as evidenced by sharp and low background LEED patterns were generated by heating and sputtering cycles. After heating to 1000 K, the crystal color changed from transparent to dark blue. This is consistent with oxygen vacancy creation in the bulk<sup>15</sup> which transforms TiO<sub>2</sub> from a wide band gap insulator to a n-type semiconductor.

Beams of 2-propanol were generated by bubbling helium through 2-propanol. We estimate the beam intensity to be approximately 0.25 ML/s (1 ML =  $5.2 \times 10^{14}$  cm<sup>-2</sup>) based on the TPD studies reported below. Mixed beams of oxygen and propanol (7:1) were generated by using O<sub>2</sub> rather than He as the carrier gas. The propanol flux in these beams is approximately 0.1 ML/s. None of the results reported below were sensitive to the ratio of oxygen to 2-propanol in the beam.

The photon source used in these studies was a 1000 W Xe lamp. A dichroic mirror was used to remove radiation with wavelengths below 280 nm and above 400 nm. The light was focused to a circle of approximately 5 mm diameter at the crystal. On the basis of measurements of the incident energy, we estimate the photon flux to be  $4 \times 10^{17}$  cm<sup>-2</sup> in the energy range 3.1–4.1 eV. (The band gap in TiO<sub>2</sub> is 3.2 eV.) This intensity is sufficient to increase the temperature of a 300 K sample by 30 K. However, the sample temperature could be stabilized in the range 200 K–800 K using a combination of liquid nitrogen cooling and sample heating.

2-Propanol and acetone were detected mass spectrometrically at masses 45 and 48, respectively, to avoid overlaps in the cracking patterns. The mass spectrometric sensitivities for acetone, 2-propanol, and water were determined from temperature-programmed desorption (TPD) experiments. TPD traces corresponding to monolayer coverage for each of these species could be identified using the appearance of a narrow physisorption peak at low temperature (see section 3.1). The integrated areas under the peaks give the relative mass spectrometric sensitivities directly.

It is thought that defects at the surface can significantly affect the reactivity of TiO<sub>2</sub>, and a variation of the defect density has been one aspect of our studies. Based on XPS<sup>16</sup> and STM<sup>17</sup> studies, a (110) oriented sample at a temperature of 850 K, exposed to an oxygen pressure of  $1 \times 10^{-6}$  Torr and cooled to 300 K in this pressure of O<sub>2</sub>, will be fully oxidized. Heating to elevated temperatures will create oxygen vacancies at the surface. Although the relationship between defect density and annealing temperature is not clear, it has been shown that heating a (110) sample in UHV to 800–1000 K will remove about 10% of the surface oxygen atoms.<sup>18</sup>

### 3. Results

#### 3.1. Adsorption and Desorption of Reactants and Products in the Absence of Light.

To provide a baseline with which to

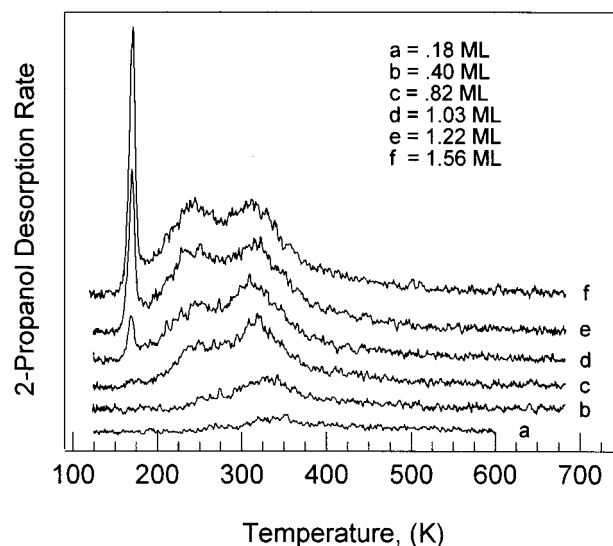


**Figure 1.** 2-Propanol desorption rate (in arbitrary units) as a function of the temperature which was increased at a rate of 7 K s<sup>-1</sup>. The curves have been offset vertically to better show the individual traces resulting from the different initial coverages shown in the figure.

compare photocatalytic activity, we have examined the interaction of reactants (2-propanol and O<sub>2</sub>) and photocatalytic oxidation products (acetone and water) with the surface in the absence of light.

**3.1.1. Oxygen.** We attempted to measure O<sub>2</sub> uptake on the surface by measuring the reflected flux in dc and modulated beam experiments and by using TPD to detect desorbing O<sub>2</sub> over the temperature range 120–700 K. TPD experiments showed a broad desorption signal peaked at 200 K which was still decreasing at 350 K. A second peak centered at 420 K, which is smaller in area by a factor of about 15, was also observed. We attribute the 200 K peak to O<sub>2</sub> weakly chemisorbed at terrace sites and the 420 K peak to molecular desorption from defect sites. The pumping speed of the detector chamber limited our modulation frequencies to greater than 1 s<sup>-1</sup>. For these frequencies, we could not detect demodulation of the O<sub>2</sub> signal between 120 and 700 K. This indicates that, at the steady-state coverages corresponding to these temperatures and beam intensities, the oxygen is bound very weakly.

**3.1.2. 2-Propanol.** Propanol was dosed onto the surface using a helium beam bubbled through 2-propanol. No reflected 2-propanol signal was observed below 125 K, indicating a unit sticking probability. A set of TPD traces for different initial coverages generated by adsorption at 125 K is shown in Figure 1. Although we have not attempted an absolute coverage determination, the appearance of a sharp peak near 170 K is a strong indication of second layer formation.<sup>19,20</sup> Using this criterion to identify completion of the monolayer ( $5.2 \times 10^{14}$  cm<sup>-2</sup>), we can say that monolayer desorption occurs from two peaks centered at 320 and 240 K. The range over which desorption occurs is 200–425 K, with a high-temperature tail extending out to 475 K.

TPD experiments following 2-propanol adsorption have been carried out previously on the {011} faceted (001) surface and on anatase and rutile powders.<sup>11–13</sup> The faceted single-crystal results are similar to ours below 375 K. However, they show a substantial second maximum near 525 K, with tails out beyond 625 K. It is not clear whether the microfaceted surface can bind 2-propanol more strongly or whether the differences are due to variations in the surface defect density. The powder studies agree well with one another and differ significantly with

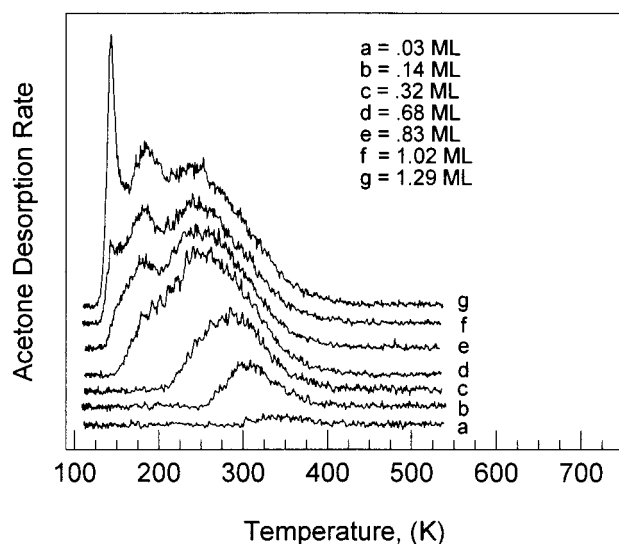


**Figure 2.** Acetone desorption rate (in arbitrary units) as a function of the temperature which was increased at a rate of  $7 \text{ K s}^{-1}$ . The curves have been offset vertically to better show the individual traces resulting from the different initial coverages shown in the figure.

our results in that desorption extends out to 600 K. No significant differences have been observed between the rutile and anatase phases.<sup>12</sup>

Previous studies of alcohols on  $\text{TiO}_2$  single-crystal faces have reported two types of adsorption-desorption behavior.<sup>11–13,20</sup> Desorption at temperatures somewhat above the multilayer peak has been attributed to molecular desorption without dissociative adsorption. Desorption at higher temperatures has been attributed to the recombination of adsorbed alkoxy and OH groups. For ethanol adsorption on  $\text{TiO}_2(110)$ , it has been shown that there are two types of ethoxy groups: one which reacts readily with surface OH groups between 250 and 400 K and a second which is unreactive below 500 K.<sup>20</sup> The ethoxy species that react between 250 and 400 K have been attributed to coordination at fully coordinated  $\text{Ti}^{4+}$  sites. The ethoxy species that reacts above 500 K has been attributed to binding at a bridging oxygen vacancy site.<sup>20</sup>

This previous work and the desorption traces in Figure 1 are consistent with the 160 and 230 K peaks originating from undissociated 2-propanol. Furthermore, the absence of any appreciable amounts of propene produced during thermal desorption of 2-propanol suggests that the 320 K peak is predominantly due to molecularly adsorbed 2-propanol. This issue will be discussed further in section 4.2.

**3.1.3. Acetone.** Thermal desorption traces for acetone are shown in Figure 2. We have assigned coverages based on associating the appearance of the sharp peak at 150 K with completion of the monolayer. Acetone desorbs at somewhat higher temperatures than 2-propanol, indicating a slightly stronger binding. Essentially all of the acetone is desorbed below 400 K, and we find no evidence of dissociative adsorption of acetone.

**3.1.4. Water.** Thermal desorption traces for water are shown in Figure 3. Our previous work<sup>16</sup> has shown that less than 2% of the water is dissociated after adsorption on  $\text{TiO}_2(110)$ , even at very low coverages. Water desorption is complete at 375 K, which is a lower temperature than that for acetone or 2-propanol.

**3.2. Thermal Reactions of 2-Propanol in the Absence of Light.** Aliphatic alcohols undergo two types of reactions on  $\text{TiO}_2$  single crystals in the absence of  $\text{O}_2$ , dehydration and

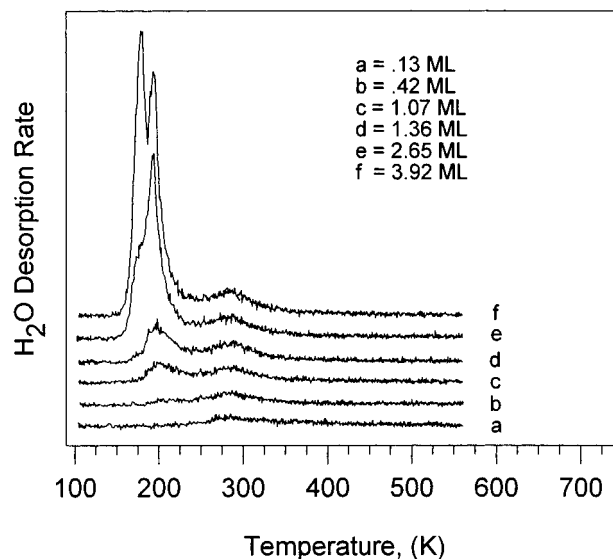


**Figure 3.** Water desorption rate (in arbitrary units) as a function of the temperature which was increased at a rate of  $7 \text{ K s}^{-1}$ . The curves have been offset vertically to better show the individual traces resulting from the different initial coverages shown in the figure.

dehydrogenation.<sup>11</sup> For 2-propanol, this leads to formation of acetone and propene. On powder samples, these products are also formed, and further decomposition to CO and  $\text{CO}_2$  is also seen.<sup>10,12,13</sup> We have observed only small amounts of decomposition products at temperatures up to 800 K. We conclude that the decomposition probability per collision with the surface is less than 0.03, with propene as the major product and acetone as a minor product.

TPD measurements for preadsorbed 2-propanol in a background pressure of oxygen have been carried out previously on powder samples. In comparison with the thermal decomposition reaction, this leads to decreased amounts of acetone and propene products and substantially increased amounts of CO and  $\text{CO}_2$ .<sup>10</sup> We have carried out similar experiments by bubbling  $\text{O}_2$  as a carrier gas through 2-propanol in the ratio  $\text{O}_2/2\text{-propanol} = 7:1$ . We observe no significant amounts of product formation beyond what is described above.

A comparison of our results with those obtained on powder samples and other orientations of single-crystalline  $\text{TiO}_2$  suggests that the (110) surface is not very effective in promoting thermal reactions of 2-propanol in either the absence or presence of  $\text{O}_2$ . More quantitatively, we conclude that the probability for dehydration, dehydrogenation, or oxidation of adsorbed 2-propanol on  $\text{TiO}_2(110)$  in the absence of light is less than 0.03.

**3.3. Photon-Induced Decomposition of 2-Propanol.** We have studied surface reactions of the 2-propanol induced by light. Experiments included long exposures of an adlayer to light followed by TPD and simultaneous exposure of a 2-propanol beam seeded in helium and the photon flux to the surface. No decomposition or oxidation of the 2-propanol was detected in either experiment. We conclude that electron-hole creation has no effect on the reactivity of adsorbed 2-propanol. A further conclusion that can be drawn from these experiments is that the reactivity of lattice oxygen, which we found to be very low in the thermal studies, is not increased through photon-induced electron-hole pair creation under these conditions. As we will discuss in section 4.2, lattice oxygen in the form of a hydroxyl group can exhibit a higher reactivity.

**3.4. Photocatalytic Oxidation of 2-Propanol with  $\text{O}_2$ .** **3.4.1. General Aspects of the Reaction.** Supplying a flux of  $\text{O}_2$  and

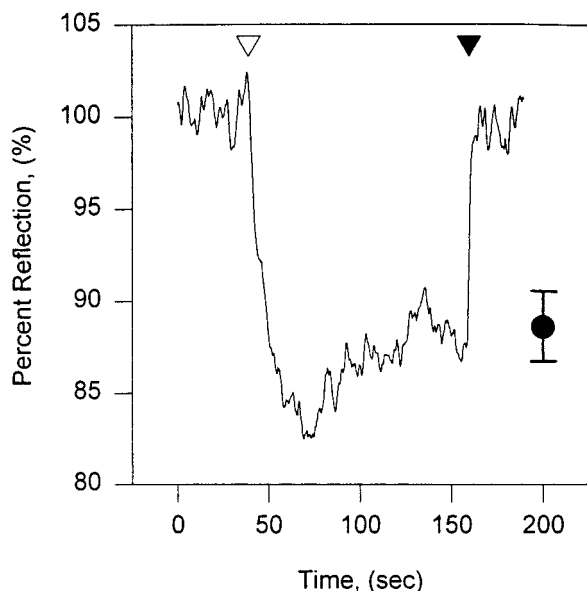


**Figure 4.** Reflected 2-propanol signal for a mixed 2-propanol/O<sub>2</sub> beam incident on the surface at steady state for  $T = 350$  K and for a preannealing temperature of 800 K. The UV light was turned on and off at times indicated by the open and filled triangles, respectively. An error bar is indicated.

2-propanol to the surface together with light (flux ratio O<sub>2</sub>:2-propanol = 7:1) leads to a significant increase in the conversion of 2-propanol to products. This can be seen both in the decrease of the reflected 2-propanol signal and in the increase of the reaction products which we observe to be acetone and H<sub>2</sub>O. Small amounts of CO<sub>2</sub> are also observed in our studies.

The reflected 2-propanol signal in a dc beam experiment is shown in Figure 4. The lamp was turned on and off at the indicated times. At steady state, essentially all of the incident 2-propanol is reflected from the surface. This signal level corresponds to a conversion efficiency of zero. Similarly, no reflected signal corresponds to a conversion efficiency of unity. Therefore, the absolute conversion efficiency of 2-propanol to reaction products can be determined directly from these data. For the particular conditions of surface preannealing temperature and reaction temperature, the conversion efficiency is 15%. This is the maximum value that has been observed. We will discuss how the conversion efficiency varies with these parameters below. The sluggish response of the signal to turning the light on and off is due to the finite desorption rate for acetone at the temperature used in this experiment.

The acetone signal obtained under similar conditions is shown in Figure 5. Until the light is turned on, no signal is observed above background. When the light is turned on, a sharp transient peak is observed which decays to a steady-state value within a few seconds. We have verified that this transient signal cannot be attributed to a temperature rise of the sample upon illumination. This was done by impinging a pure acetone beam onto the surface while modulating the light beam. No synchronous acetone desorption waveform which would have resulted from a modulation of the surface temperature was seen. We have verified that the transient signal cannot be attributed to photodesorption of acetone by the same method. In this case a synchronous waveform would be obtained for which the degree of demodulation is temperature-independent. Fragmentation of a parent 2-propanol molecule in the ionizer as a cause of the signal can be ruled out because we used mass 58, at which there is no 2-propanol cracking product, to monitor the acetone signal.

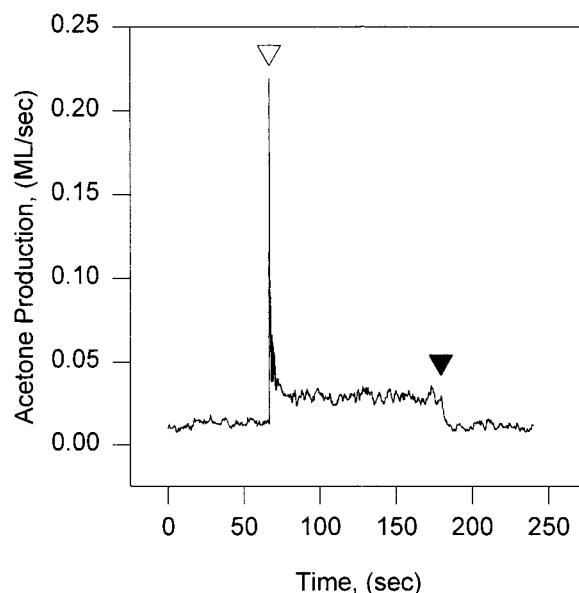


**Figure 5.** Acetone production rate as a function of time for a surface preannealed to 800 K. A very sharp transient peak which decays to a steady-state regime is seen. The UV light was turned on and off at times indicated by the open and filled triangles, respectively.

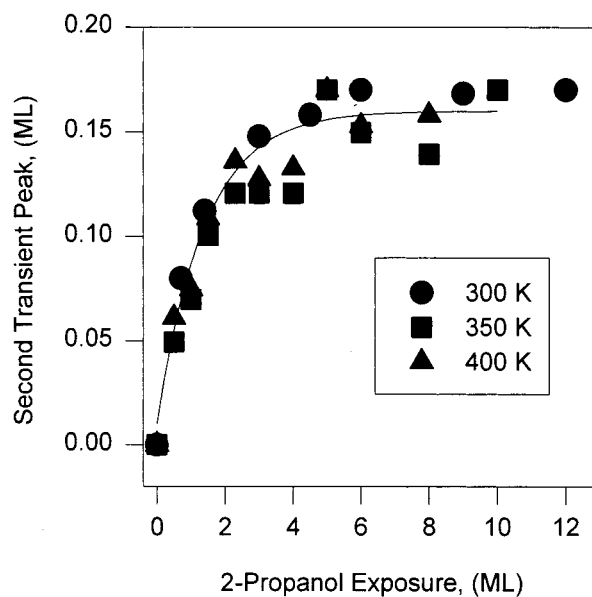


**Figure 6.** Acetone coverage corresponding to the second of two successive transient peaks as a function of exposure to the beam between the two experiments. The slope is a measure of the effective sticking coefficient (see text).

The origin of the transient peak can be understood on the basis of the experiments summarized in Figure 6. We carried out the experiment shown in Figure 5 twice in succession and incrementally increased the time between individual light exposures. During these experiments, the reactant beam remained on the entire time and the photon flux was off in the variable time period. As shown in Figure 6, we found that the transient peak height depends on the time for which the surface is exposed to the reactant flux with the photon flux off. By contrast, the steady-state rate of acetone production is unchanged.

As can be seen in Figure 6, an integrated beam flux corresponding to 4 monolayers of propanol (and an excess of O<sub>2</sub> corresponding to ~30 monolayers) is required to saturate the transient peak. The initial rise corresponds to an effective



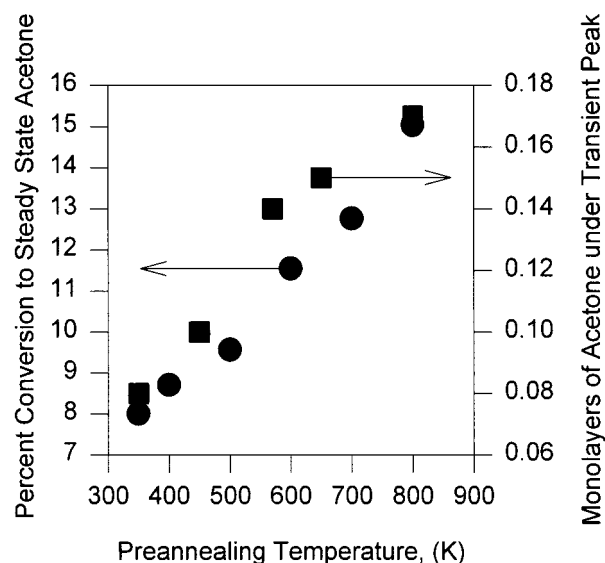
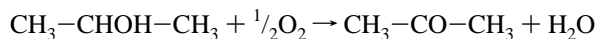


**Figure 7.** Measures of the steady-state and transient conversion of 2-propanol to acetone as a function of the preannealing temperature.

reactive sticking coefficient of 0.12. This suggests that the transient peak is due to a saturation of the surface with adsorbed  $O_2$  and propanol in the absence of light. When the light is turned on, conversion to acetone occurs very fast, leading to a depletion of surface reactants. After this occurs, the steady-state reaction rate is limited by the beam intensity rather than by the rate of the photochemical reaction. This leads to a sharp decrease in the acetone signal and a leveling off to the steady-state value. The integrated area under the transient peak is a measure of the fractional saturation coverage that can react to form acetone, and the steady-state rate is a measure of the rate of uptake of the reactants, 2-propanol and  $O_2$ . As can be seen in Figure 6, the results are unaffected by significant changes in the surface temperature. This indicates that the sticking coefficients for the reactants are temperature-independent over this range.

**3.4.2. Water Production in the Photocatalytic Oxidation of 2-Propanol.** Water is formed in this reaction, and we find that a transient signal is also observed in the water product signal. With the appropriate choice of a scaling factor, the acetone and water transient signals can be superimposed. This shows that acetone and water are formed in the same rate-limiting reaction. As discussed above, the TPD data can be used to convert the mass spectrometric signals for 2-propanol, acetone, and water into absolute coverages. Under the reaction conditions used,  $250\text{ K} < T < 600\text{ K}$ , we find that the ratio of acetone to water production is  $1.0 \pm 0.1:1$ . This is the predicted ratio for the reaction



The observed product ratio suggests that there are no other major reaction channels that we have overlooked.

**3.4.2. Effect of Surface Preannealing Temperature on the Conversion Efficiency of 2-Propanol to Acetone.** It is well-known that heating  $TiO_2$  in a vacuum leads to a depletion of oxygen in the surface and near-surface region.<sup>15</sup> Pan et al.<sup>18</sup> have shown that up to 10% of the surface oxygen can be removed upon annealing in a vacuum at 800 K. Yates and co-workers have shown that preannealing increases the photocatalytic activity for CO oxidation.<sup>21</sup> We show in Figure 7 that preannealing also has a significant effect for the oxidation of 2-propanol. The steady-state conversion efficiency of a surface

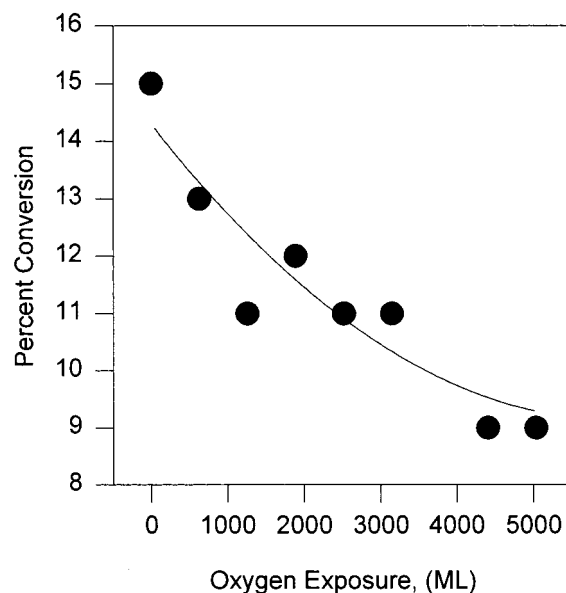


**Figure 8.** Dependence of the steady-state conversion of 2-propanol to acetone as a function of exposure time to the beam with the UV light on. The beam has a flux of 0.1 and 0.7  $ML\ s^{-1}$  in 2-propanol and oxygen, respectively. The solid line represents the trend of the data.

preannealed at 800 K is nearly a factor of 2 greater than for a fully oxidized surface. Both the area under the transient peak and the steady-state conversion efficiency are affected to the same degree by the preannealing temperature as is expected from the explanation of the transient peak discussed above.

However, as is shown in Figure 8, the higher values of conversion efficiency are not stable in an oxidizing environment. Prolonged exposure to the 2-propanol/oxygen beam leads to a decrease in conversion efficiency from 15% to 9% after an exposure of approximately  $5 \times 10^3$  monolayers of  $O_2$ . As we have shown previously in the case of water adsorption/desorption from this surface,<sup>16</sup> reoxidation of the surface occurs quickly. However, oxygen vacancies in the near surface region are quite resistant to reoxidation. We note that the residual activity for a fully oxidized surface is less than a factor of 2 below that for a surface with a considerable density of oxygen vacancies. Although the presence of defects leads to a higher reactivity, the photocatalytic reactivity is already quite high for a fully oxidized surface.

**3.4.3. Effect of Surface Temperature on Conversion Efficiency.** The conversion efficiency of 2-propanol to acetone and water is strongly temperature-dependent. The same dependence on temperature is observed for the transient and steady-state acetone signals and for the water signal as is shown in Figure 9. All of this is consistent with the interpretation for the transient peak given above and for the simultaneous or near simultaneous evolution of acetone and water after the rate-limiting step. The conversion efficiency is near zero below 200 K and above 600 K. It is sharply peaked in this range with a maximum near 350 K.

The origin of the low conversion efficiency at low temperatures could be either a low desorption rate for acetone or a low conversion rate to form acetone from 2-propanol at low temperatures. We have clarified this issue by exposing the surface to the  $O_2$ /2-propanol beam at various initial temperatures for a time sufficient to generate a coverage of approximately 1 monolayer of 2-propanol. With the beam off, the  $TiO_2(110)$  sample was illuminated for a fixed time, and the conversion efficiency was subsequently determined using TPD by monitoring the 2-propanol and acetone evolved upon heating. These

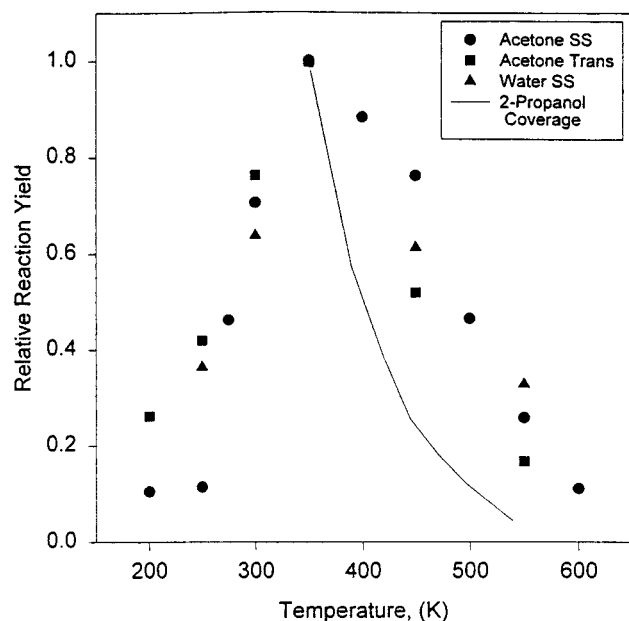


**Figure 9.** Relative reaction yield of acetone as a function of temperature. The signals for the steady-state and transient acetone production and for water production have been normalized to the same value at 350 K. The solid line shows the behavior expected at high temperatures if the temperature dependence of the yield were determined by the temperature dependence of the total 2-propanol coverage.

experiments showed that the conversion efficiency was independent of temperature between 120 and 350 K. This shows that the activation energy for the photocatalytic reaction is very small. We conclude that the apparent decrease in conversion efficiency seen in Figure 9 below 350 K is in fact due to a rate-limiting desorption of acetone, rather than to a decrease in the dehydrogenation rate.

The form of the conversion efficiency versus temperature curve at high temperatures could be due to the decrease in the surface coverages of either adsorbed 2-propanol or O<sub>2</sub>. The predicted decrease in the 2-propanol coverage with increasing temperature can be calculated by integrating the area under the TPD traces shown in Figure 1. The results of this calculation, normalized to the acetone production at 350 K, is also shown as a solid line in Figure 9. The observed lack of agreement between the rate of acetone production and the 2-propanol coverage suggests that the decrease in the adsorbed oxygen coverage, rather than the decrease in the 2-propanol coverage, is responsible for the falloff in conversion efficiency for  $T > 350$  K. This result is consistent with the measurements of Yates et al.,<sup>22</sup> who concluded that molecular oxygen was stable on the TiO<sub>2</sub>(110) surfaces up to 400 K. However, as we will show in section 3.4.4, only strongly bound 2-propanol reacts to form acetone in the photocatalytic reaction. Because this fraction of the adsorbed 2-propanol also desorbs in the range 300–400 K, these TPD experiments do not give conclusive evidence on which of the two reactant coverages limits the conversion efficiency at temperatures above 350 K.

#### 3.4.4. Kinetics of the Photocatalytic Oxidation of 2-Propanol.

The kinetics of the reaction have been studied by obtaining waveforms for reactants and products upon modulating the mixed 2-propanol/O<sub>2</sub> beam while using a time-independent light intensity, as well as by modulating the light while using a time-independent reactant beam intensity. These two measurements give complementary information. The response time of the acetone signal to modulating the reactant beam with a time-independent light flux is a combination of the relaxation time

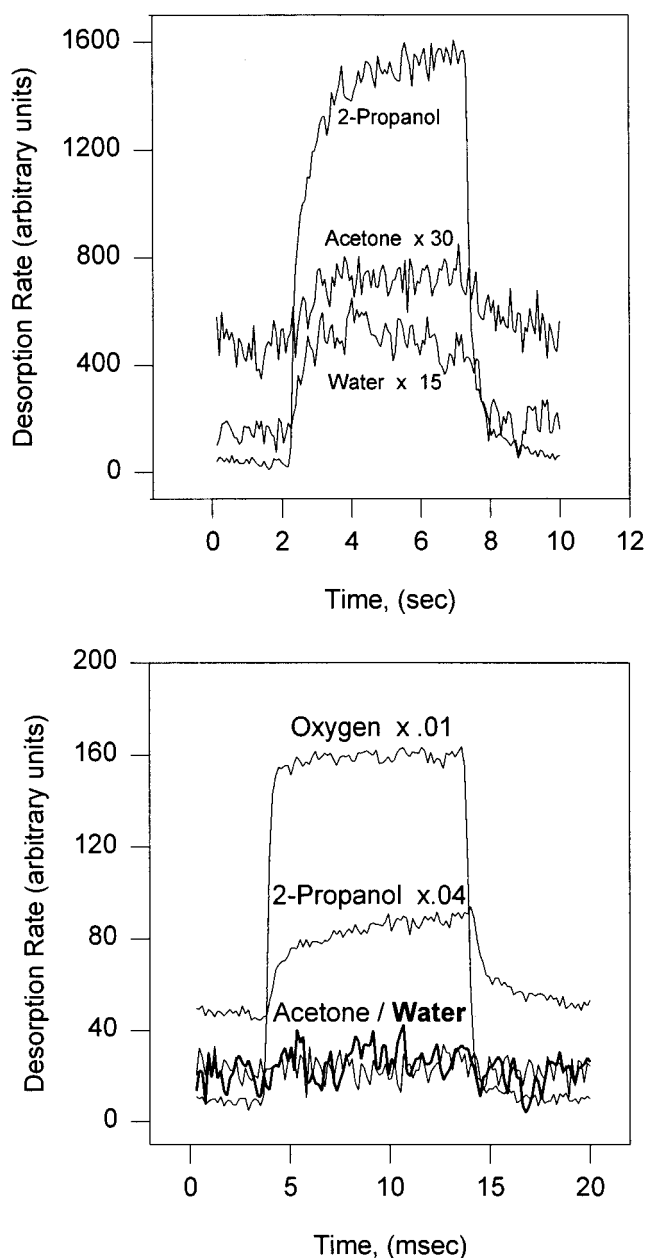


**Figure 10.** Waveforms for reactants and products for modulation frequencies of 0.1 (a) and 50 s<sup>-1</sup> (b). All curves have the same zero. The presence of a background signal near  $t = 0$  is indicative of a residence time long in comparison with the inverse of the modulation frequency.

of the reactant coverage and the residence time of the desorbing acetone. By contrast, the response time of the acetone signal to modulating the light flux with a time-independent reactant flux is a combination of the relaxation time for the photochemical reaction and the residence time of the desorbing acetone.

The time response of reactants and products at a surface temperature of 350 K for modulating the beam at 50 s<sup>-1</sup> and 0.1 s<sup>-1</sup> while keeping the light intensity constant is shown in Figure 10. At both modulation frequencies, the O<sub>2</sub> scattered flux has essentially no dc component. This shows that the scattered O<sub>2</sub> flux corresponds to molecules that are very weakly adsorbed on the surface. Their residence time will satisfy the relationship  $\tau \ll 1/\omega$ . The 2-propanol flux shows roughly equal dc and ac components at 50 s<sup>-1</sup>. This shows that there is a significant variation in 2-propanol binding energies as is reflected in the TPD results shown in Figure 1. This means that for some of

the 2-propanol molecules  $\tau \ll 1/\omega$ , whereas for others,  $\tau \gg 1/\omega$ . Even at  $0.1 \text{ s}^{-1}$ , the 2-propanol signal shows a significant degree of demodulation. This is a further illustration of the wide range of binding energies for 2-propanol on single-crystalline  $\text{TiO}_2(110)$ . The acetone and water signals have no ac component at  $50 \text{ s}^{-1}$ , showing that for these species  $\tau \gg 1/\omega$ .

This last result indicates that at  $50 \text{ s}^{-1}$  acetone and water production originates *only* from the 2-propanol that is totally demodulated. It allows us to conclude that acetone production in the photochemical reaction comes *only* from strongly bound 2-propanol which we can associate with the 320 K peak in Figure 1. Previous studies<sup>11–13,20</sup> have indicated that this peak may be attributed to dissociatively adsorbed molecules. However, on the basis of the absence of propene production in the thermal decomposition of 2-propanol in the absence of oxygen and band gap radiation, we believe that the degree of dissociation in this peak is small. This issue will be discussed further in section 4.2. Figure 10 shows that, even for a chopping frequency of  $0.1 \text{ s}^{-1}$ , both ac and appreciably demodulated acetone and water signals are observed. This shows that the 2-propanol which reacts to form acetone and water exhibits a very wide range of surface binding energies.

The results obtained by using a dc beam and modulating the light are quite different. The acetone waveforms obtained for modulation of the light flux show a negligible degree of demodulation at 350 K, even for a chopping frequency of  $50 \text{ s}^{-1}$ . The variation of the waveform amplitude with temperature is identical to waveforms obtained for acetone scattered from the  $\text{TiO}_2(110)$  surface in the absence of band gap radiation. We conclude from this result that the photochemical reaction to form acetone is fast compared to the desorption of acetone.

**3.4.5. What Fraction of the Surface Sites Are Active in the Photooxidation of 2-Propanol?** We have shown above that a single collision of 2-propanol with a preannealed surface can lead to a conversion efficiency to acetone of 15% for a preannealed surface. The efficiency is reduced to 9% upon long-term exposure to the beam, presumably due to the reoxidation of oxygen vacancies. This raises the question of whether the conversion efficiency is a measure of the reactivity of normal lattice sites or the area average of a small number of highly reactive surface sites and a large number of unreactive sites.

We have investigated this question by immobilizing an adsorption layer generated with the mixed  $\text{O}_2$ /2-propanol beam at 185 K and irradiating it for various amounts of time. The acetone and 2-propanol coverages are subsequently measured using TPD. The 2-propanol coverage is reduced through desorption and reaction in this experiment. The acetone production is shown in Figure 11. It exhibits an initial rapid rise and a subsequent slow increase. The slope of this curve is proportional to the quantum yield. From the known photon flux and acetone coverage, we determine the initial quantum yield to be  $4 \times 10^{-6}$ . This quantum yield is several orders of magnitude lower than what has been determined for photocatalytic reactions on colloidal particles.<sup>23,24</sup> It indicates that, on semiinfinite single-crystal surfaces, electron–hole recombination is highly probable. Recombination may be enhanced by the preannealing, which creates bulk oxygen vacancies.

The saturation value for long light exposures shows that no more than 0.17 ML of acetone can be produced from a reactant saturated surface. Since the adlayer is immobile at 185 K, we conclude that the entire acetone production is due to approximately 15% of the surface sites for a surface preannealed to 800 K. This number is consistent with estimates<sup>18</sup> on the

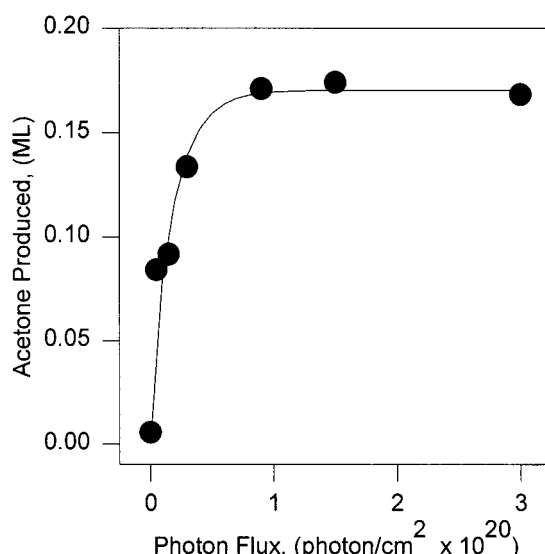


**Figure 11.** Acetone produced as a function of time exposed to the UV light incident on a immobile mixed 2-propanol/ $\text{O}_2$  adlayer of approximately 1 ML for an illumination temperature of 180 K.

oxygen vacancy density. This result suggests that normal lattice sites on  $\text{TiO}_2(110)$  are unreactive in the photooxidation of 2-propanol using molecular oxygen and that the 8% reactivity for a fully oxidized surface is due to defects such as steps. Comparing the average reactivity of the preannealed surface (17%) with the fraction of surface sites active in the reaction (15%) allows us to conclude that those sites which are reactive have near-unity reactivity. The same reasoning holds for the fully oxidized surface.

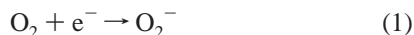
## 4. Discussion

**4.1. What Adsorbed Species Are Involved in the Photochemical Dehydrogenation of 2-Propanol to Acetone?** The results presented above show that the transformation does not take place unless both light and oxygen are supplied to the surface. This shows that the lattice oxygen in  $\text{TiO}_2(110)$  is unreactive with 2-propanol in the absence of  $\text{O}_2$  even under illumination with band gap radiation. Since dissociatively adsorbed oxygen should be identical to lattice oxygen which we have shown to be unreactive, we conclude that molecularly bound oxygen is involved in the reaction. However, as we discuss below, lattice oxygen in the form of OH groups may be reactive. We were unable to quantify the coverage of reactive  $\text{O}_2$  through TPD experiments, because an appreciable fraction of this species dissociates and reacts with excess Ti from the bulk rather than desorbing. Based on the data discussed in section 3.4.5, the minimum coverage of reactive  $\text{O}_2$  must be 0.075 ML. This estimate is based on the observed maximum water coverage of 0.15 ML and the stoichiometric ratio of 2 between  $\text{H}_2\text{O}$  and  $\text{O}_2$ .

The reactive  $\text{O}_2$  has two roles in 2-propanol conversion to acetone. It provides oxygen atoms to form  $\text{H}_2\text{O}$  and/or to replace lattice oxygen used to form  $\text{H}_2\text{O}$ . In addition, it has the role of trapping electrons. Because the reaction does not proceed without light, it must be initiated by electron–hole pair excitation and subsequent trapping of one of these by a surface species. We observe that no reaction occurs when only adsorbed 2-propanol is present on the illuminated surface. Therefore, 2-propanol and lattice oxygen at the surface do not create an imbalance between electrons and holes needed to initiate a redox reaction. As it is well established that the  $\text{O}_2$  molecule is a



good electron scavenger,<sup>1</sup> the initial reaction under our reaction conditions is most likely to be



in which the superoxide ion radical is formed.

The modulated reactant beam studies show that only strongly bound 2-propanol undergoes dehydrogenation to acetone. An upper limit to the coverage of the reactive 2-propanol is given by the area of the high-temperature peak in the TPD data shown in Figure 1, which is 0.4 ML. Measurements of 2-propanol adsorption on TiO<sub>2</sub> single crystals and powders<sup>10,12,13</sup> as well as other aliphatic alcohols<sup>20</sup> indicate that, for the systems investigated to date, a significant fraction of the monolayer is dissociatively adsorbed. In all cases in which dissociation has been shown to occur, a dehydration product has also been observed. Although the detection of a dehydration product is a sensitive measure of the degree of dissociation of the adsorbed alcohol, the branching ratio between dehydration and dehydrogenation depends on the OH and H<sub>2</sub>O surface concentration.<sup>10,12,13</sup> This makes it difficult to quantify the degree of 2-propanol dissociation in this work. However, the absence of propene production in the range 600–750 K in this work suggests that the reactive strongly bound 2-propanol is predominantly nondissociatively adsorbed at Ti<sup>4+</sup> sites on the surface.

**4.2. Why Does the TiO<sub>2</sub>(110) Surface Support Dehydrogenation in a Photochemical Reaction But Not in a Thermal Reaction?** A number of studies have demonstrated that differently oriented TiO<sub>2</sub> single crystals can have significantly different reactivities. Water is readily dissociated on the (100) surface<sup>25</sup> but not on the (110) surface.<sup>16,26</sup> The reactions of small organic molecules on TiO<sub>2</sub> single crystals show a strong dependence on surface orientation.<sup>27</sup> These differences are not understood in detail, but Barteau and co-workers<sup>27</sup> have convincingly argued that major trends in reactivity can be understood in terms of the availability of differently coordinated sites at the surface. With this in mind, it is instructive to compare the thermal and photochemical results obtained in this work with previous studies by Barteau and co-workers of the thermal reaction on {011} faceted TiO<sub>2</sub>(001).

For 2-propanol adsorption on {011} faceted TiO<sub>2</sub>(001), Kim and Barteau<sup>11</sup> found that approximately 44% of the 2-propanol is desorbed in a low-temperature peak centered at 360 K. Other than water, no reaction products are observed in this temperature range. The remaining 56% of the initially adsorbed 2-propanol is desorbed as propene and 2-propanol in approximately equal amounts in a high-temperature peak centered at 510 K. By contrast, we find that on TiO<sub>2</sub>(110) no more than 3% of the adsorbed 2-propanol is converted to propylene and no 2-propanol is desorbed above 400 K. Acetone, which is the dehydrogenation product, is not observed in either thermal reaction study. However, on {011} faceted TiO<sub>2</sub>(001), the dehydrogenation products from 1-propanol, methanol, and ethanol are all formed at the high temperature at which dehydration occurs.

It appears that thermally induced chemical transformations of the adsorbed 2-propanol are linked to a very strongly bound propoxy species. It has been proposed by Gamble et al.<sup>20</sup> that, for ethylene production from adsorbed ethanol (which occurs near 650 K) on TiO<sub>2</sub>(110), the reaction products formed at high temperature are linked to an ethoxy species in which the oxygen occupies a bridging oxygen vacancy site, rather than being coordinated to an in-plane Ti<sup>4+</sup> site. Such vacancy sites can be produced through the associative desorption of two OH

groups on the surface which occurs at temperatures near 300 K.<sup>20</sup> The hydrogen in these OH groups originates from the dissociation of the alcohol, but the oxygen is a lattice oxygen. Therefore, the associative desorption leads to vacancy formation. However, vacancy formation by this mechanism requires a significant degree of dissociation of the adsorbed alcohol to create the OH groups that can recombine. Gamble et al.<sup>20</sup> observed that half of the dissociated ethanol recombined to form ethanol in the gas phase, and half was converted to ethylene. If we assume that the same degree of partitioning applies to our system, the 3% conversion of 2-propanol to propylene seen in this work suggests that no more than 6% of the propoxy groups are bound at bridging oxygen vacancy sites and, therefore, that no more than 6% of the adsorbed 2-propanol is dissociatively adsorbed. As we do not know the branching ratio for our system, we regard this estimate of the degree of dissociation as a lower limit. The propoxy groups bound at bridging oxygen vacancy sites are not likely to be the species that produce acetone photocatalytically in our experiment, because the fractional coverage of 6% is significantly less than the observed photochemical conversion efficiency of 15%. Therefore, the photochemical conversion of 2-propanol to acetone appears to originate from a different adsorbed state than that seen by Kim and Barteau.<sup>11</sup> This is the basis for our attribution (see section 4.1) of the photochemical reactivity predominantly to undissociated 2-propanol molecules coordinated at Ti<sup>4+</sup> sites.

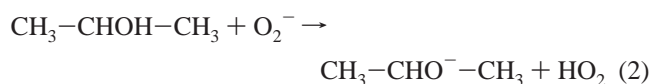
As has been shown recently, the strongly bound propoxy species can also be made to yield acetone in a thermal reaction. Rekoske and Barteau<sup>13</sup> have recently studied the thermal conversion of 2-propanol on oxidized anatase powders between 450 and 600 K. They find that the selectivity to produce acetone rather than propylene at a given temperature or degree of conversion can be significantly increased by the addition of O<sub>2</sub> or H<sub>2</sub>O to the gas mixture passed over the catalyst. This observation is consistent with dehydrogenation being favored only if the surface is somewhat reduced. Rekoske and Barteau<sup>13</sup> suggest that acetone formation occurs through an  $\alpha$ -abstraction reaction between an alkoxide and a hydroxyl group bound to the same Ti cation. Such sites may be available on powders but are apparently not present on the TiO<sub>2</sub>(110) plane or on {011} faceted TiO<sub>2</sub>(001).

It is clear that the acetone observed in this study is produced in a different mechanism than the thermal reaction. Whereas acetone is desorbed near 510 K on {011} faceted TiO<sub>2</sub>(001), we observe acetone production at 180 K. This is consistent with a free-radical reaction for which the activation energy is negligible.

These considerations lead us to the following mechanistic possibilities. Unless indicated otherwise, all species indicated in the equations below are adsorbed on the surface. In an initial step, light leads to electron–hole pair creation. Some electrons are trapped by an adsorbed O<sub>2</sub>.

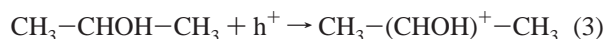


The superoxide ion radical is not a sufficiently strong base to remove either the hydrogen on the OH group or the hydrogen bound to the tertiary carbon.<sup>28</sup> The pK<sub>a</sub> values for 2-propanol and O<sub>2</sub>H are 18 and 5, respectively,<sup>29</sup> so that H<sup>+</sup> abstraction as outlined in eq 2 below is unlikely to proceed.

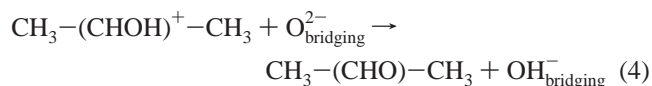




Electron trapping by molecular oxygen allows excess holes to be trapped by the 2-propanol.



This greatly reduces the barrier to removing an  $\text{H}^+$

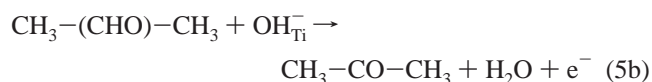


Because the molecule is bound to the surface through the oxygen, the OH bond will be weakened, which may lead to preferential removal of this hydrogen. This is consistent with the observation that dissociation of alcohols on  $\text{TiO}_2$  surfaces occurs by removal of the OH hydrogen,<sup>10,12,13,20</sup> even though the C–H bond is weaker than the O–H bond.<sup>30</sup>

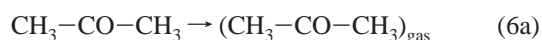
The remaining hydrogen on the reaction intermediate is easily removed by an hydroxide group to give acetone and water in a single step. Subsequent desorption of the products into the gas phase will be quasi-simultaneous because, as seen in Figures 2 and 3, both species desorb in the same temperature range. We propose



or



in which vac designates a bridging oxygen vacancy, followed by

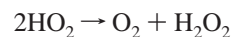


The reaction could take place with either type of hydroxide group thought to be present on  $\text{TiO}_2$ . A hydroxide group coordinated to a Ti site is indicated by  $\text{OH}_{\text{Ti}}^-$ . Such groups could be produced from  $\text{O}_2^-$  through surface intermediates such as  $\text{HO}_2^-$  as well as through interconversion between  $\text{OH}_{\text{Ti}}^-$  and  $\text{OH}_{\text{bridging}}^-$ .<sup>20</sup>

If the water is formed from  $\text{OH}_{\text{bridging}}^-$ , then lattice oxygen will appear in the product. If the water is formed from  $\text{OH}_{\text{Ti}}^-$ , the origin of the oxygen in the product is the incident gas-phase molecule. Isotopic labeling experiments could be used to distinguish between these two possibilities. Although  $\text{OH}_{\text{bridging}}^-$  are generally called acidic groups and are primarily thought of as sources of  $\text{H}^+$ , it has been shown that water can be formed through a recombination of two  $\text{OH}_{\text{bridging}}^-$  at temperatures as low as 250 K.<sup>20,31</sup> This suggests that the formation of the OH bond considerably weakens the bond between a bridging lattice oxygen and its coordination shell of Ti cations. As discussed by Gamble and Campbell,<sup>20</sup> the interconversion of  $\text{OH}_{\text{bridging}}^-$  and  $\text{OH}_{\text{Ti}}^-$ , which occurs in the temperature range of interest, may make the outcome of a labeling experiment less clear-cut.

An alternate mechanism could be proposed in which the initial step is hydrogen abstraction from adsorbed 2-propanol by OH

radicals formed from  $\text{O}_2^-$  through reactions such as<sup>28</sup>



The species  $\text{HO}_2$ ,  $\text{HO}_2^-$ ,  $\text{H}_2\text{O}_2$ , and OH are all capable of initiating redox reactions, and rapid interconversion between these species can occur. This may make it difficult to identify one surface species as dominant. A mechanism involving the OH radical would also explain the fact that acetone is the major product observed in this work. Reaction of OH with 2-propanol in the gas phase<sup>32</sup> or in the aqueous phase<sup>33</sup> results almost exclusively in hydrogen abstraction from the tertiary carbon. However, the observed lack of dissociation of 2-propanol has the consequence that there are very few hydroxide groups present at the onset of the reaction. Given our evidence that the reactive 2-propanol is predominantly undissociated, a mechanism in which OH radicals play a predominant role is unlikely. After hole trapping and an initial hydrogen abstraction (eqs 3 and 4), a second hydrogen can be easily removed from the reaction intermediate. This removal (eq 5) could be accomplished by either a hydroxide group or a hydroxyl radical. However, this does not alter our hypothesis that the initial step is hole trapping by adsorbed and undissociated 2-propanol.

The mechanism proposed in eqs 1–6 is consistent with the observation that water and acetone production have the same time signature. The primary function of the gas-phase molecular oxygen in this mechanism is to scavenge electrons, allowing hole trapping by the 2-propanol to proceed. If the removal of the second hydrogen occurs preferentially through  $\text{OH}_{\text{bridging}}^-$ , the gas-phase oxygen has the secondary function of replenishing the lattice oxygen. The mechanism is also consistent with our observation that the reactivity enhancement brought about by the creation of oxygen lattice vacancies is not immediately lost. If the mechanism proceeds through  $\text{OH}_{\text{bridging}}^-$ , new vacancies are created as product molecules are evolved. Although some of these will be oxidized by  $\text{O}_2$  and  $\text{O}_2^-$ , they will not be immediately depleted. If the reaction proceeds through  $\text{OH}_{\text{Ti}}^-$ , the original vacancies remain and are only slowly oxidized through  $\text{O}_2$ .

**4.3. What Sites Support the Dehydrogenation of 2-Propanol on  $\text{TiO}_2(110)$ ?** The experiments outlined in section 3.4.5 show that the fraction of surface sites that support the reaction ranges between 0.08 for a fully oxidized surface and 0.15 for a surface that has been preannealed to 800 K in a vacuum. Since this fraction is significantly less than one, one can conclude that normal lattice sites are not active for this reaction. The increase in reactivity upon preannealing in a vacuum is quantitatively consistent with the increase expected in the concentration of surface oxygen vacancies. ISS experiments have shown<sup>18</sup> that up to 10% of the surface oxygen can be removed to generate vacancies through preannealing to 800 K.

This would seem to suggest a critical role for oxygen vacancies in this reaction. However, vacancies produced through preannealing will be reoxidized if the surface is exposed to  $\text{O}_2$  as shown in Figure 8 or to water as we have shown previously.<sup>16</sup> Therefore, we do not expect surface oxygen vacancies to provide the basis for catalytic activity in an oxidizing environment. As Figure 8 shows, even under the modest reactant flux achievable with our experimental methods,

the surface reactivity decreases to that expected for a fully oxidized surface quite rapidly.

The requirements for surface reactivity are that the surface coverage of the reactants are sufficiently high to result in a reasonable rate, that the state of the adsorbed reactants is appropriate to promote reactivity, and that not all electron-hole pairs recombine. Our experiments show that the 2-propanol coverage can be quite high under reaction conditions but that only the strongly bound fraction is reactive. Oxygen is more weakly bound and is reactive only in the molecular state. The electron-hole recombination rate is very high, but this does not limit the reaction rate at the light and reactant flux levels used in this work. The increased reactivity for the preannealed surface may be due to an increased oxygen coverage or greater degree of dissociation of 2-propanol due to stronger binding at oxygen vacancy sites. However, it may also be due to small changes in the probability for electron-hole recombination due to the presence of the vacancies. The reactivity for the fully oxidized surface is high enough to question whether oxygen vacancies are truly necessary to induce activity in photocatalytic reactions. Our work suggests that the inherent heterogeneity present even on metal oxide single-crystal surfaces, coupled with the favorable location of the energies of the conduction and valence band edges relative to the Fermi level of the system, is sufficient to promote photocatalytic activity on TiO<sub>2</sub>.

These results show that although oxygen vacancies enhance the photocatalytic activity, the enhancement is only a factor of 2. However, we have previously shown that although water will rapidly reoxidize surface defects, XPS still shows emission in the Ti<sup>3+</sup> region after long exposure to water at 300 K.<sup>16</sup> This is indicative of subsurface defects that may be difficult to reoxidize even at atmospheric pressure or in aqueous solutions. Such defects may be the direct or indirect basis for the residual activity we see for a fully oxidized surface. This suggests that there may be a variety of local environments that facilitate reactivity through either increased binding of a reactant or enhanced trapping of an electron or hole produced through band gap radiation.

## 5. Conclusions

We conclude that the TiO<sub>2</sub>(110) surface is relatively unreactive in the thermal conversion of small oxygen-containing molecules such as alcohols because it is not effective in dissociating these molecules to form strongly bound reactive intermediates such as those in which an alkoxy oxygen occupies an oxygen vacancy site. However, if free-radical intermediates are generated on the surface through light, reactions that are observed on rutile and anatase TiO<sub>2</sub> powders can occur with significant probability at much lower temperatures. Our work suggests that photochemical dehydrogenation, which is the dominant reaction pathway observed for 2-propanol, is initiated after electron trapping by molecular oxygen through a hole trapping mechanism.

**Acknowledgment.** This work was supported by the Chemistry Division of the National Science Foundation. We have greatly benefited from discussions with Charles Campbell, Karen Goldberg, and James Mayer.

## References and Notes

- (1) Helz, G. R.; Zepp, R. G.; Crosby, D. G. *Aquatic and Surface Photochemistry*; Helz, G. R., Zepp, R. G., Crosby, D. G., Eds.; Lewis Publishers: Boca Raton, FL, 1994.
- (2) Mills, A.; Hunte, S. L. *J. Photochem. Photobiol. A: Chem.* **1997**, *108*, 1–35.
- (3) Kesselman, J. M.; Weres, O.; Lewis, N. S.; Hoffmann, M. R. *J. Phys. Chem. B* **1997**, *101*, 2637–2643.
- (4) Cermenati, L.; Pichat, P.; Guillard, C.; Albini, A. *J. Phys. Chem. B* **1997**, *101*, 2650–2658.
- (5) Schwartz, P. F.; Turro, N. J.; Bossmann, S. H.; Braun, A. M.; Wahab, A. A.; Durr, H. *J. Phys. Chem. B* **1997**, *101*, 7127–7134.
- (6) Bahnemann, D. W.; Hilgendorff, M.; Memming, R. *J. Phys. Chem. B* **1997**, *101*, 4265–4275.
- (7) Linsebigler, A. L.; Lu, G.; J. T. Yates, J. *Chem. Rev.* **1995**, *95*, 735–758.
- (8) Lu, G.; Linsebigler, A.; J. T. Yates, J. *J. Phys. Chem.* **1995**, *99*, 7626–7631.
- (9) Linsebigler, A.; Lu, G.; J. T. Yates, J. *J. Chem. Phys.* **1995**, *103*, 9438–9443.
- (10) Larson, S. A.; Widegren, J. A.; Falconer, J. L. *J. Catal.* **1995**, *157*, 611–625.
- (11) Kim, K. S.; Barteau, M. A. *J. Mol. Catal.* **1990**, *63*, 103–117.
- (12) Lusvardi, V. S.; Barteau, M. A.; Farneth, W. E. *J. Catal.* **1995**, *153*, 41–53.
- (13) Rekoske, J. E.; Barteau, M. A. *J. Catal.* **1997**, *165*, 57–72.
- (14) Farrall, P. D.; Engel, T. *Rev. Sci. Instrum.* **1996**, *67*, 4027–4028.
- (15) Henrich, V. E.; Cox, P. A. *The Surface Science of Metal Oxides*; Cambridge University Press: Cambridge, 1994.
- (16) Brinkley, D.; Dietrich, M.; Engel, T.; Farrall, P.; Gantner, G.; Schafer, A.; Szuchmaker, A. *Surf. Sci.* **1998**, *395*, 292–306.
- (17) Szabo, A.; Engel, T. *Surf. Sci.* **1995**, *329*, 241–254.
- (18) Pan, J. M.; Maschoff, B. L.; Diebold, U.; Madey, T. E. *J. Vac. Sci. Technol. A* **1992**, *10*, 2470.
- (19) Hugenschmidt, M. B.; Gamble, L.; Campbell, C. T. *Surf. Sci.* **1994**, *302*, 329–340.
- (20) Gamble, L.; Jung, L. S.; Campbell, C. T. *Surf. Sci.* **1996**, *348*, 1–16.
- (21) Linsebigler, A.; Lu, G.; J. T. Yates, J. *J. Phys. Chem.* **1996**, *100*, 6631–6636.
- (22) Lu, G.; Linsebigler, A.; J. T. Yates, J. *J. Chem. Phys.* **1994**, *102*, 4657–4662.
- (23) Serpone, N. *J. Photochem. Photobiol. A: Chem.* **1997**, *104*, 1–12.
- (24) Tahiri, H.; Serpone, N.; Mao, R. L. v. *J. Photochem. Photobiol. A: Chem.* **1996**, *93*, 199–203.
- (25) Henderson, M. A. *Surf. Sci.* **1994**, *319*, 315.
- (26) Henderson, M. A. *Surf. Sci.* **1996**, *355*, 151.
- (27) Idriss, H.; Barteau, M. A. *Catal. Lett.* **1994**, *26*, 123–139.
- (28) Bielski, B. H. J.; Cabelli, D. E.; Arudi, R. L. *J. Phys. Chem. Ref. Data* **1985**, *14*, 1041.
- (29) Ouellette, R. J.; Rawn, J. D. *Organic Chemistry*; Prentice Hall: Englewood Cliffs, NJ, 1996.
- (30) Lide, D. R. *CRC Handbook of Chemistry and Physics*; 78th ed.; Lide, D. R., Ed.; CRC Press: Boca Raton, FL, 1997.
- (31) Henderson, M. A. *J. Phys. Chem. B* **1997**, *101*, 221–229.
- (32) Atkinson, R. *J. Phys. Chem. Ref. Data* **1989**, *1*, 1.
- (33) Dorfman, L. M.; Adams, G. E. *Natl. Stand. Ref. Data Ser., Natl. Bur. Stand. (US)* **1973**, *41*, 1.